Development of a fluorescent nanosensor for ribose

Ida Lager[a], Marcus Fehr[a,b], Wolf B. Frommer[a,b,*], Sylvie Lalonde[a]

[a] *ZMBP Tübingen, Plant Physiology, Auf der Morgenstelle 1, D-72076 Tübingen, Germany*
[b] *Carnegie Institution, 260 Panama St., Stanford, CA 94305, USA*

Received 6 August 2003; revised 22 August 2003; accepted 22 August 2003

First published online 9 September 2003

Edited by Felix Wieland

Abstract To analyze ribose uptake and metabolism in living cells, nanosensors were engineered by flanking the *Escherichia coli* periplasmic ribose binding protein with two green fluorescent protein variants. Following binding of ribose, fluorescence resonance energy transfer decreased with increasing ribose concentration. Five affinity mutants were generated covering binding constants between 400 nM and 11.7 mM. Analysis of nanosensor response in COS-7 cells showed that free ribose accumulates in the cell and is slowly metabolized. Inhibitor studies suggest that uptake is mediated by a monosaccharide transporter of the GLUT family, however, ribose taken up into the cell was not or only slowly released, indicating irreversibility of uptake.

Key words: Nanosensor; Ribose; Fluorescence resonance energy transfer; Transport

1. Introduction

D-Ribose is a component of RNA, DNA, ATP, and many co-factors, as well as a potential source of energy. Before entering metabolism ribose is phosphorylated to D-ribose-5-phosphate, a precursor for nucleotide, histidine, and tryptophan synthesis. Ribose-5-phosphate is a normal intermediate of the hexose monophosphate shunt, but free ribose may appear as an intermediate of nucleotide metabolism. Pentoses serve as nutrients in ruminants and may be relevant as dietary supplement [1,2]. In eukaryotes, little is known about both uptake and metabolism of ribose and it is not known whether significant amounts of free ribose are present in the cytosol.

Ribose is required for the biosynthesis of basic biomolecules such as nucleotides and the amino acids tryptophan and histidine. Endogenous ribose is available from glucose via the hexose monophosphate shunt. In many tissues endogeneous ribose is available from glucose via the hexose monophosphase shunt. However, tissues with low hexose monophosphate activity depend on ribose recycling and on alternative ribose sources [2]. Ribose can be released from nucleosides during metabolic turnover and nucleosides can be transported across the plasma membrane [3,4]. However, when endogenous nucleotides are degraded and lost from tissues the ability to replenish nucleotide pools appears to be limited by the supply of ribose [2].

Utilization of external ribose for nucleobase salvage and repletion of cellular adenine nucleotide levels require transport of ribose across the plasma membrane. To date, only limited information about ribose transport is available. Rat hepatoma cell lines may use ribose as sole carbon source indicating that mammalian cells possess the ability to take up ribose [5]. Competition studies using 3-*O*-methylglucose and ribose were performed with a number of tissues leading to different results: no significant inhibition of 3-*O*-methylglucose uptake into isolated rat hepatocytes was observed in the presence of ribose [6]. Similarly, 3-*O*-methylglucose uptake into *Cyprinus carpio* was not affected by ribose [7] indicating that ribose and glucose do not compete for transport in these tissues. However, in primary cultures of bovine brain microvessel endothelial cells, 3-*O*-methylglucose uptake was competitively inhibited by ribose [8]. In addition to transport across the plasma membrane, ribose uptake into rat liver lysosomes and competition with glucose could be directly demonstrated using radiolabelled sugars suggesting subcellular compartmentalization of ribose [9]. Ribose is phosphorylated by a specific ribokinase, a protein not directly related to hexokinases [10], and although the bacterial homolog has been characterized in very much detail [11], little is known about the properties of the mammalian homolog.

To analyze ribose transport in mammalian cells a fluorescence resonance energy transfer (FRET)-based ribose sensor was generated by flanking the *Escherichia coli* periplasmic ribose binding protein (RBP) with two green fluorescent protein (GFP) variants. As shown recently, the substrate-induced FRET change between two GFP variants attached to the *E. coli* periplasmic maltose binding protein (MBP) can be used to visualize maltose uptake into living yeast [12]. Similarly, glucose dynamics in green African monkey-derived COS-7 cells were visualized using an *E. coli* periplasmic glucose/galactose binding protein (GGBP) fused between to GFP variants [13]. RBP and GGBP share approximately 21% sequence identity and both belong to type I periplasmic binding proteins [14,15]. Comparison of the crystal structures of *E. coli* RBP and GGBP show that many structural features are conserved between the two proteins [16–18]. Ribose nanosensors (fluorescent indicator protein-ribose (FLIPrib)) were developed by fusing GFP variants to the RBP termini. Consistent with the expected relative movement of the fluorescent proteins upon binding of ribose to FLIPrib, FRET efficiency decreased. To perform ribose measurements at a wide range

*Corresponding author.
E-mail address: frommer@andrew2.stanford.edu (W.B. Frommer).

Abbreviations: DMEM, Dulbecco's modified Eagle's medium; FLIP, fluorescent indicator protein; FRET, fluorescence resonance energy transfer; GGBP, glucose galactose binding protein; MBP, maltose binding protein; RBP, ribose binding protein

0014-5793/03/$22.00
doi:10.1016/S0014-5793(03)00976-1

of concentrations potential residues important for binding were selected and five affinity mutants were generated. To detect ribose in the cytosol of mammalian cells and visualize ribose transport FLIPribs were expressed in COS-7 cells. Addition of extracellular ribose led to increased cytosolic ribose levels visualizing ribose transport. Ribose uptake was sensitive to inhibitors for glucose transporters (GLUT) such as cytochalasin B and phloretin and to glucose suggesting that ribose and glucose transport into the cytosol of COS-7 cells are mediated by the same transport protein.

2. Materials and methods

2.1. FLIPrib constructs and plasmids

A RBP polymerase chain reaction product from genomic *E. coli* DNA encoding mature RBP was cloned into the KpnI site of FLIPglu-600μ in pRSETB [13] (Invitrogen) replacing the glucose sensor's mglB moiety and transferred into BL21(DE3)Gold (Stratagene). For expression in COS-7 cells the chimeric gene was inserted into pCDNA3.1 (Invitrogen). The RBP sequence was confirmed by DNA sequencing and was found to carry a $D_{208}G$ substitution. Since $D_{208}G$ did not significantly affect the binding affinity (see Table 1), all further experiments were carried out with the nanosensor named FLIPrib-250n carrying $D_{208}G$. Mutant forms carrying substitutions $T_{135}A$, $Q_{235}A$, $F_{15}A$, $F_{16}A$ and $R_{141}A$ were generated using QuikChange (Stratagene) in the mutant background of FLIPrib-250n. FLIPrib proteins were extracted from BL21(DE3)gold and purified as described [12].

2.2. In vitro characterization of FLIPrib

Substrate titration curves and substrate specificity analyses were performed on Safire (Tecan) fluorometer. ECFP was excited at 433 nm and emission was set to 475 nm and 528 nm for ECFP and EYFP, respectively. All in vitro analyses were performed in 20 mM sodium phosphate buffer at pH 7. FRET was determined as EYFP–ECFP emission intensity ratio. Using the change in ratio upon ligand binding, binding constants (K_d) were determined by fitting substrate titration curves to:

$$S = 1-(r-r_{min})/(r_{max}-r_{min}) =$$

$$[S]_b/[P]_t = n[S]/(K_d + [S]) \quad (1)$$

where $[S]$ is substrate concentration, $[S]_b$ concentration of bound substrate, n number of binding sites, $[P]_t$ total concentration of binding protein, r ratio, r_{min} minimum ratio in absence of ligand, r_{max} maximum ratio at saturation. Hill coefficients were determined using the Hill equation:

$$S = (n[S]^n)/(K_d + [S]^n) \quad (2)$$

2.3. Cell culture and transfection

COS-7 cells were grown in Dulbecco's modified Eagle's medium (high glucose; DMEM, Biochrom) with 10% fetal calf serum and 50 U/ml penicillin and streptomycin (Biochrom). Cells were cultured at 37°C and 5% CO_2. For imaging, cells were cultured in 8-well tissue culture glass slides (BD Falcon) and transiently transfected at 50–70% confluence using Lipofectamine/Plus Reagent (Invitrogen). Transfection efficiency as determined by counting fluorescing cells was at least 30%.

2.4. Imaging

Imaging was performed 35–40 h after transfection on a fluorescence microscope (DMIRB, Leica) with a cooled CCD camera (Sensys Photometrics). Dual emission intensity ratios were recorded using Metafluor 4.5 (Universal Imaging) with 436/20 excitation and two emission filters (480/40 for ECFP and 535/30 for EYFP) and neutral density filter (1% transmission) for excitation. Images were acquired within the linear detection range of the camera at intervals of 20–30 s for up to 90 min. Depending on expression level, exposure times varied between 0.75 and 1.5 s. If not mentioned otherwise, cells were perfused with glucose-free DMEM (Sigma) at flow rates of 1.8 ml/min in a chamber with a total volume of 0.7 ml. Inhibition of transporters of the GLUT family was performed with 2 μM cytochalasin B or 100 μM phloretin (Sigma). Phloridzin (Sigma) at a concentration of 100 μM was used for inhibition of Na^+-dependent glucose transporters (SGLTs). In a large number of experiments, variation of the initial ratio (±5%) at the beginning of an experiment was observed. This does not seem to reflect differences in sugar levels, but rather variability in optical parameters when measuring individual cells. Analyses were repeated at least three times with similar results.

3. Results and discussion

3.1. Construction of a ribose sensor

Mature RBP was flanked with two GFP variants by attaching a cyan (CFP) and a yellow fluorescent protein (YFP) to the N- and C-terminus, respectively. Due to the relative position of the termini to the hinge region of RBP the ribose-induced hinge-twist motion is predicted to move the GFP variants further apart and to cause a decrease in FRET. Titration of the purified fusion protein FLIPrib-250n displayed a ribose concentration-dependent decrease in FRET. The binding constant (K_d) for ribose was determined by FRET as 250 nM with a maximum change in ratio of 0.19 (Table 1) and a Hill coefficient of 0.93. The YFP-CFP emission intensity ratio was similar to the ratio of the GGBP-based glucose sensors reflecting the three-dimensional similarity of RBP and GGBP [13,16,17]. FLIPrib-250n permits ribose quantification in the high-affinity range between 0.03 and 2.3 μM.

3.2. Affinity mutants of FLIPrib

To perform ribose measurements across a broader range of concentrations, affinity mutants of FLIPrib-250n were generated. RBP binds its substrate by hydrogen bonding and stacking forces between aromatic amino acid residues [16]. Using data from the crystal structure of RBP [16], and a table of predicted residues conserved in a variety of periplasmic bind-

Table 1
Properties of the nanosensors

Nanosensor	Mutant form[a]	K_d	Range for quantification[b]	Δr_{max} [c]
FLIPrib-250n		0.25 ± 0.03 μM	0.028–2.29 μM	0.19
FLIPrib-400n	$T_{135}A$	0.40 ± 0.04 μM	0.044–3.60 μM	0.30
FLIPrib-4μ	$Q_{235}A$	4.29 ± 0.26 μM	0.48–38.6 μM	0.36
FLIPrib-120μ	$F_{15}A$	119 ± 8.68 μM	13.2–1068 μM	0.29
FLIPrib-3m	$F_{16}A$	2.90 ± 0.31 mM	0.32–26.1 mM	0.37
FLIPrib-12m	$R_{141}A$	11.7 ± 0.48 mM	1.30–105 mM	0.38

[a]All FLIPribs carry the amino acid substitution $D_{208}G$. As expected, the affinity of FLIPrib-250n seems almost unchanged as compared to wild type RBP with 0.13 μM determined by other methods [20].
[b]Range of concentrations for which a nanosensor can be used. The range for quantification was defined as the range between 10% and 90% saturation.
[c]Δr_{max}, in vitro maximum change in ratio between absence and saturation of the binding protein.

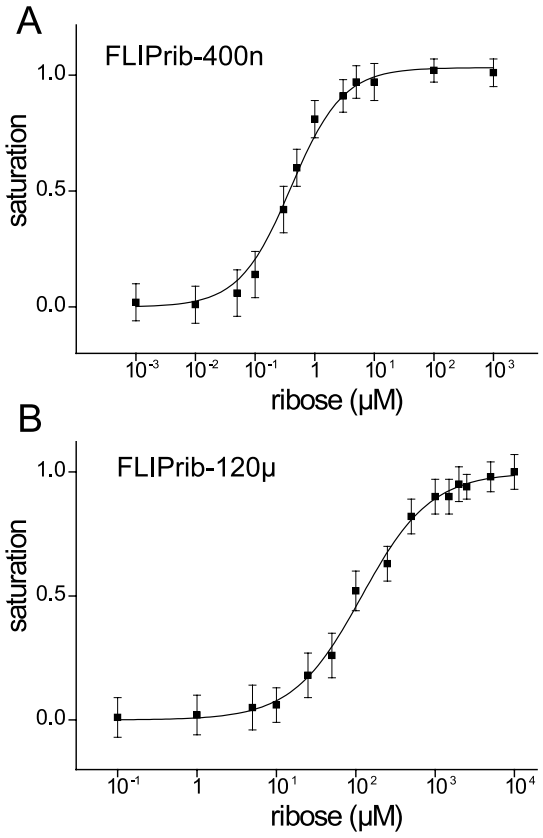

Fig. 1. In vitro substrate-induced FRET changes of purified nanosensors. Saturation curves were obtained by transforming the ribose-dependent ratio change into saturation of the sensor. Using non-linear regression the K_ds of FLIPrib-400n (A) and FLIPrib-120μ (B) were determined as 400 nM and 120 μM, respectively. The saturation curves represent titrations of three independent protein extracts.

ing proteins, we selected five residues for site-directed mutagenesis [19]. Mutation of positions corresponding to amino acids in the binding site of RBP in FLIPrib-250n produced a set of ribose sensors covering a broad range of ribose levels (Table 1). Introducing substitution $T_{135}A$ into the RBP moiety of FLIPrib-250n produced FLIPrib-400n, which has a binding constant (K_d) of 0.4 μM for ribose, thus providing a range for ribose quantification between at least 0.04 and 3.60 μM (Table 1, Fig. 1A). The small change was expected, since T_{135} does not seem to be involved in hydrophobic interactions with the substrate directly, although it is in the vicinity of the binding site [16]. However, the $T_{135}A$ change led to a higher maximal change in ratio, probably by affecting the overall movement. Due to its higher maximum ratio change between absence and saturation with ribose (Δr_{max}) of 0.3, FLIPrib-400n permits more sensitive measurements than FLIPrib-250n at low ribose concentrations (Table 1). The Hill coefficient was determined as 1.03, consistent with the formation of a 1:1 FLIPrib-400n/ribose complex. F_{15} and F_{16} are involved in hydrophobic interactions with ribose, whereas Q_{235} and R_{141} are involved in hydrogen bonding of hydroxyl groups at positions 2 and 3 of ribose. The K_d of 119 μM of FLIPrib-120μ, carrying a $F_{15}A$ substitution, permits ribose measurements between 13 μM and 1 mM (Table 1, Fig. 1B). As for FLIPrib-400n, Δr_{max} of FLIPrib-120μ (0.29) is higher than Δr_{max} of FLIPrib-250n (Table 1). Together with

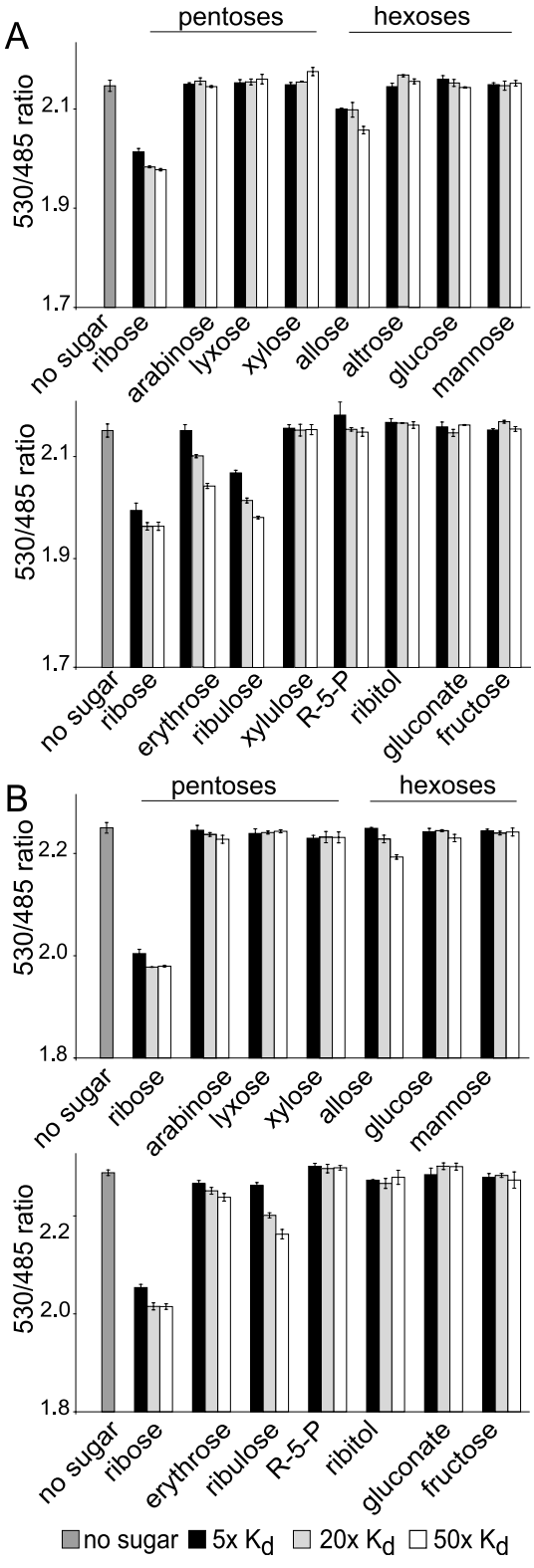

Fig. 2. Comparison of substrate selectivity of two FLIPrib variants. The ratio changes of purified FLIPrib-250n (A) and FLIPrib-120μ (B) were determined in the presence of various pentoses and hexoses at three different concentrations (5, 10 and 50 times the K_d). Apart from ribose, allose, erythrose and ribulose were recognized by the sensors (R-5-P, ribose-5-phosphate).

FLIPrib-4μ, which has a K_d of 4.29 μM for ribose covering a range from 0.5 to 40 μM, FLIPrib-120μ permits ribose quantifications at intermediate levels of ribose. FLIPrib-3m and FLIPrib-12m carrying substitutions $F_{16}A$ and $R_{141}A$, respectively, with affinities in the millimolar range (FLIPrib-3m, 2.9 mM and FLIPrib-12m, 11.7 mM) are suitable for ribose quantification in the low to high millimolar range (Table 1). Because of its high K_d, FLIPrib-12m was used as a control sensor for measurements in COS-7 cells. Together with FLIPrib-4μ the Δr_{max} values of FLIPrib-3m (0.37) and FLIPrib-12m (0.38) provide the highest sensitivity of all six ribose sensors.

3.3. Substrate specificity

Determination of substrate concentration in complex mixtures, i.e. the cytoplasm of living cells, requires sensors that display high specificity toward their substrate. To analyze which sugars are recognized by two of the variants, FLIPrib-250n (Fig. 2A) and FLIPrib-120μ (Fig. 2B) were incubated with different sugars. Substrate-induced conformational changes were measured using FRET in microplate assays. Consistent with the ability of RBP to bind allose 1000 times less tightly than ribose [20], FLIPrib-250n binds allose at high concentrations (Fig. 2). Besides allose, only ribulose and erythrose were recognized by FLIPrib-250n and FLIPrib-120μ (Fig. 2). Erythrose was recognized by FLIPrib-250n at a concentration of 50 times the K_d for ribose (50% of the ratio change at saturation with ribose). In contrast, ribulose was bound by FLIPrib-250n at concentrations as low as 5 times the K_d of ribose (30% of the ratio change at saturation with ribose). Interestingly, ribulose did not interfere with binding of ribose to the pure RBP as had been measured by Aksamit and Koshland [20]. For FLIPrib-120μ the ratio change induced by erythrose at 50 times the K_d of ribose was 20% of the maximum ratio change observed for ribose. The ratio change for ribulose at 5 times the K_d was 10% of the maximum ratio change. All other sugars, including ribose-5-phosphate, did not induce any significant decrease in ratio. Overall, FLIPrib-120μ has slightly higher substrate specificity than FLIPrib-250n. FLIPribs can thus be considered specific ribose sensors suitable for in vivo imaging.

3.4. Ribose transport and detection of ribose in the cytosol of COS-7 cells

To show that ribose can be transported across the plasma

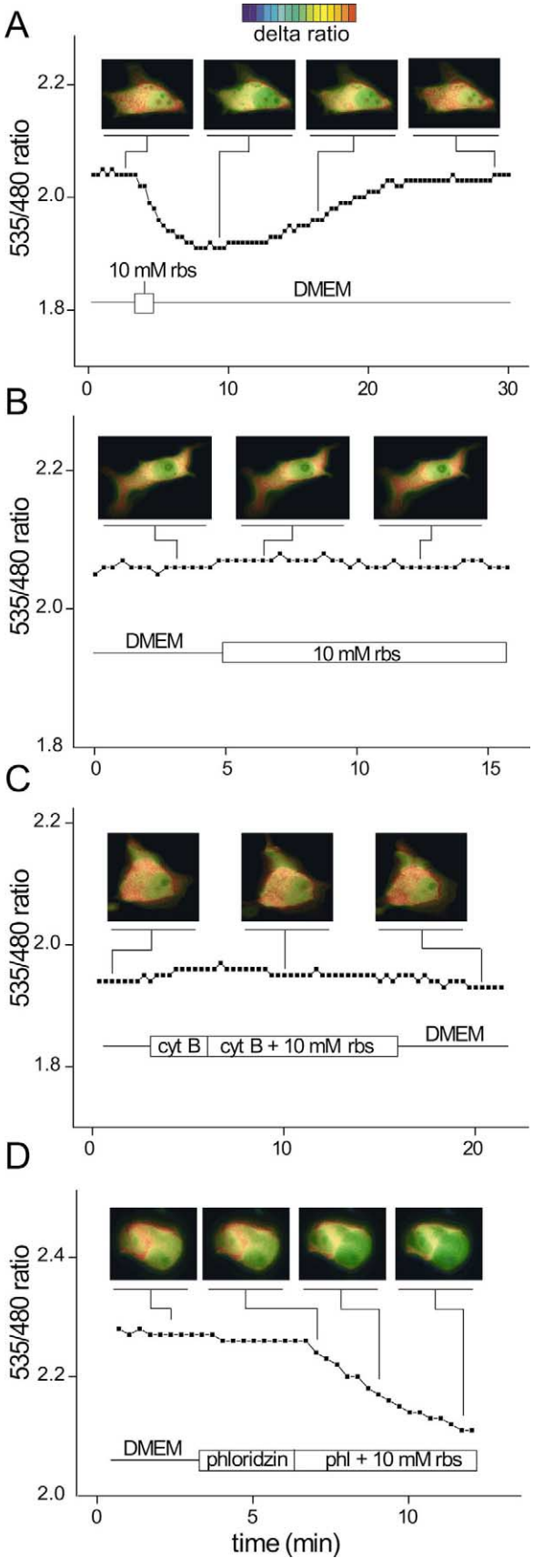

→

Fig. 3. Ribose transport and detection of ribose in the cytosol of COS-7 cells. Ratio images are pseudo-colored to demonstrate ribose-dependent ratio changes. Red indicates high ratio and blue indicates low ratio. Integration of the ratio over entire cells was used to quantify the ratio change. Each graph shows ratio changes for a single cell. Addition of ribose to COS-7 cells led to a decrease in ratio. A: After removal of ribose from FLIPrib-120μ-expressing cells the ratio returned to the starting value showing reversible binding of ribose. B: Addition of ribose to FLIPrib-12m-expressing cells did not lead to a decrease in the ratio making the sensor useful as a control sensor. C: In the presence of 2 μM cytochalasin B, ribose uptake into cells expressing FLIPrib-120μ was inhibited, suggesting that ribose is transported by a member of the GLUT family. D: Phloridzin, an inhibitor of SGLT glucose transporters, did not inhibit transport of ribose and consequently a change in ratio for FLIPrib-120μ was observed. Glucose-free DMEM was used to remove external ribose and inhibitors.

membrane of mammalian cells, FLIPrib-120μ and, as a control, FLIPrib-12m were expressed in the cytosol of cultured Green African monkey kidney-derived COS-7 cells. Emission intensity images of COS-7 cells were acquired microscopically by excitation at 436 nm and high speed switching between emission filters for YFP and CFP using a CCD camera. Ratio images were calculated on a pixel-by-pixel basis. To quantify the ratios obtained by microscopical imaging, data were integrated over entire cells. Merged YFP-CFP emission intensity images showed expression of the FLIPrib sensors in the cytosol but neither in the polyploid nuclei nor in lysosomes. Following addition of external ribose to the cells, the emission intensity ratio decreased indicating transport of ribose across the plasma membrane (Fig. 3A), and demonstrating that the sensor is functional in vivo. Similar results were obtained with FLIPrib-400n (data not shown). To study re-export or to follow metabolism of ribose in the cytosol, ribose was removed by perfusion with ribose-free medium following addition of ribose and ribose detection inside the cytosol. After washing out ribose the emission intensity ratio increased slowly to its starting ratio, showing that binding to RBP in vivo is reversible (Fig. 3A). The return to baseline was slow compared to results obtained for glucose metabolism in COS-7 cells with glucose sensors [13]. The difference in kinetics together with the seeming absence of glucose re-export from COS-7 cells observed previously suggests that the return to baseline is due to slow metabolism of ribose. Ribokinase, an enzyme involved in phosphorylation of ribose, might be responsible for the metabolism. The absence of a change in ratio when using FLIPrib-12m as control sensor demonstrates that the responses observed in the cells are specific and that cytosolic levels remain comparatively low in the cytosol (Fig. 3B). To further substantiate that the decrease in the ratio after addition of ribose was due to ribose binding, glucose was added as a control to the FLIPrib-120μ sensor. After addition of glucose no change in ratio was observed (results not shown), consistent with the in vitro specificity of the sensor. When a mixture of glucose and ribose was added, uptake rates were slower compared to uptake of ribose alone (data not shown), suggesting that ribose might be transported into the cell by a glucose transporter. To test this hypothesis further, COS-7 cells were perfused with cytochalasin B, an inhibitor of GLUT activity. When a mixture of cytochalasin B and ribose was added to the cell, uptake of ribose was inhibited (Fig. 3C), suggesting that ribose is transported by a member of the GLUT family. Phloretin, another inhibitor of GLUT activity, also inhibited ribose uptake although not completely (data not shown). Finally, uptake was insensitive to phloridzin, an inhibitor of SGLT glucose transporters, consistent with the absence of SGLT1 in COS-7 cells [21]. This study together with a recent report on the development of chemically modified periplasmic binding proteins [22] demonstrates that many of the periplasmic binding proteins can be developed into nanosensors for a wide range of analytes. This assumption is supported by the fact that RBP and GGBP are only approximately 21% identical. Furthermore, although at the primary sequence level RBP and GGBP are basically unrelated to MBP, all three can be used to generate FRET-based nanosensors using the same strategy. Despite the difference in primary sequence, all proteins share similar tertiary structures, and the proteins can be grouped into two structural subfamilies (types) [15], in which the respective termini are located in different relative positions. In all cases the direction of FRET change is consistent with the predicted relative movement of the fluorescent moieties. Furthermore, the availability of FLIPrib nanosensors represents the basis for generating a wide spectrum of nanosensors for other compounds by computational design [19] as exemplified by design of RBPs binding trinitrotoluene or lactate [23]. In summary, the third example of a nanosensor for in vivo imaging on the basis of periplasmic binding proteins establishes the general applicability of this approach and provides a new tool that might help towards a better understanding of the mechanisms of ribose transport and metabolism in the contexts of nucleotide metabolism and the use of ribose as a dietary nutrient.

Acknowledgements: We thank Rama Panford Walsh and Felicity de Courcy for critical reading of the manuscript. The project was supported by grants from the Deutsche Forschungsgemeinschaft (Nichtinvasive Imaging Verfahren für Metaboliten), Gottfried-Wilhelm Leibniz award and Fonds der Chemischen Industrie.

References

[1] Scharrer, E. and Grenacher, B. (2000) J. Vet. Med. A Physiol. Pathol. Clin. Med. 47, 617–626.
[2] Pauly, D.F., Johnson, C. and St Cyr, J.A. (2003) Med. Hypotheses 60, 149–151.
[3] Mercader, J., Gomez-Angelats, M., del Santo, B., Casado, F.J., Felipe, A. and Pastor-Anglada, M. (1996) Biochem. J. 317, 835–842.
[4] Patil, S.D. and Unadkat, J.D. (1997) Am. J. Physiol. 272, G1314–G1320.
[5] Jargiello, P. (1980) Biochim. Biophys. Acta 632, 507–516.
[6] Elliott, K.R., Bate, A.J. and Craik, J.D. (1984) Int. J. Biochem. 16, 1251–1253.
[7] Teerijoki, H., Krasnov, A., Pitkanen, T.I. and Molsa, H. (2001) Comp. Biochem. Physiol. B Biochem. Mol. Biol. 128, 483–491.
[8] Takakura, Y., Kuentzel, S.L., Raub, T.J., Davies, A., Baldwin, S.A. and Borchardt, R.T. (1991) Biochim. Biophys. Acta 1070, 1–10.
[9] Maguire, G.A., Docherty, K. and Hales, C.N. (1983) Biochem. J. 212, 211–218.
[10] Bork, P., Sander, C. and Valencia, A. (1993) Protein Sci. 2, 31–40.
[11] Sigrell, J.A., Cameron, A.D. and Mowbray, S.L. (1999) J. Mol. Biol. 290, 1009–1018.
[12] Fehr, M., Frommer, W.B. and Lalonde, S. (2002) Proc. Natl. Acad. Sci. USA 99, 9846–9851.
[13] Fehr, M., Lalonde, S., Lager, I., Wolff, M.W. and Frommer, W.B. (2003) J. Biol. Chem. 278, 19127–19133.
[14] Shilton, B.H., Flocco, M.M., Nilsson, M. and Mowbray, S.L. (1996) J. Mol. Biol. 264, 350–363.
[15] Fukami-Kobayashi, K., Tateno, Y. and Nishikawa, K. (1999) J. Mol. Biol. 286, 279–290.
[16] Mowbray, S.L. and Cole, L.B. (1992) J. Mol. Biol. 225, 155–175.
[17] Mowbray, S.L. (1992) J. Mol. Biol. 227, 418–440.
[18] Vyas, N.K., Vyas, M.N. and Quiocho, F.A. (1991) J. Biol. Chem. 266, 5226–5237.
[19] Johnson, J.M. and Church, G.M. (2000) Proc. Natl. Acad. Sci. USA 97, 3965–3970.
[20] Aksamit, R.R. and Koshland Jr., D.E. (1974) Biochemistry 13, 4473–4478.
[21] Birnir, B., Lee, H.S., Hediger, M.A. and Wright, E.M. (1990) Biochim. Biophys. Acta 1048, 100–104.
[22] de Lorimier, R.M. et al. (2002) Protein Sci. 11, 2655–2675.
[23] Looger, L.L., Dwyer, M.A., Smith, J.J. and Hellinga, H.W. (2003) Nature 423, 185–190.